Coherent photon bremsstrahlung and dynamics of heavy-ion collisions: Comparison of different models

U. Eichmann,[1] C. Ernst,[1] L. M. Satarov,[2] and W. Greiner[1]
[1]*Institut für Theoretische Physik, J. W. Goethe-Universität, D-60054 Frankfurt am Main, Germany*
[2]*The Kurchatov Institute, RU-123182 Moscow, Russia*
(Received 17 December 1999; published 1 September 2000)

Differential spectra of coherent photon bremsstrahlung in relativistic heavy-ion collisions are calculated within various schematic models of the projectile-target stopping. Two versions of the degradation length model, based on a phenomenological deceleration law, are considered. The simple shock wave model is studied analytically. The predictions of these models agree in the soft photon limit, where the spectrum is determined only by the final velocity distribution of charged particles. The results of these models in the case of central Au+Au collisions at the AGS bombarding energy are compared with the predictions of the microscopic transport model UrQMD. The latter model is also used to calculate photon spectra at SIS, SPS, and RHIC energies. It is shown that at the AGS energy the coherent photon bremsstrahlung exceeds the photon yield from π^0 decays at c.m. photon energies $\omega \lesssim 50$ MeV.

PACS number(s): 25.75.−q, 13.40.−f

I. INTRODUCTION

Real photon bremsstrahlung emitted in the course of a heavy-ion collision may provide information about the underlying dynamics and the stopping law of nuclear matter. To understand the sensitivity of photon spectra to the dynamics of a heavy-ion collision, it is instructive to compare the predictions of models based on different dynamical scenarios of the collision process. In earlier publications the coherent bremsstrahlung was studied in phenomenological [1–8] as well as microscopical [9] models. In the present paper we concentrate on the comparative analysis of different models, which has not been done in the above-mentioned works.

In Sec. II some general properties of bremsstrahlung spectra common to all models are obtained from basic considerations about the nature of coherent bremsstrahlung. Section III introduces different deceleration models: a shock wave model and a degradation length model both with and without consideration of the transverse extension of the colliding nuclei. In addition we employ a microscopic transport model which is not restricted to the initial deceleration stage. The comparison of these models is performed in Sec. IV.

A serious problem in observing the coherent photon bremsstrahlung is the large background of $\pi^0 \to \gamma\gamma$ decays. It is especially strong at ultrarelativistic bombarding energies (AGS and higher). To overcome this problem it was suggested [5,7] to study experimentally sufficiently soft photons (with energies less than several MeV in the case of RHIC). According to our calculation the contribution of the π^0 decays is indeed relatively small at low photon energies. This problem is studied in more detail in Sec. IV. Conclusions and discussion are given in Sec. V.

II. GENERAL DISCUSSION

In this section some general model-independent properties of bremsstrahlung spectra are discussed. According to the Larmor formula the energy spectrum of the bremsstrahlung is proportional to the squared absolute value of the Fourier transformed force $f(t)$ acting on a charge [10], $dI/d\omega \sim |f(\omega)|^2$. From general properties of the Fourier transformation one is led to a number of conclusions.

(1) At large photon energies the radiated energy tends to zero if the force is absolutely integrable. In contrast, instantaneous interactions (δ forces) generate a flat energy spectrum. The latter approximation is valid in the so-called soft-photon limit ($\omega \to 0$), which in turn can be interpreted as a limit $\tau \to 0$ where τ is the interaction time.

(2) From the scaling behavior of Fourier transforms it may be shown that the bremsstrahlung drops the faster in ω the longer the force acts on the charge (this is the analogue of Heisenberg's uncertainty principle). As a result, the energy spectra of bremsstrahlung photons become harder in the collision of smaller nuclei or at higher bombarding energies.

(3) If the force $f(t)$ is essentially nonzero in a finite time interval $|t| \leqslant a$, which is a common assumption in all models describing heavy-ion collisions far above the Coulomb barrier, the spectra of bremsstrahlung photons exhibit oscillations in ω. Indeed, any continuous function on a finite interval can be approximated with arbitrary accuracy by a polynomial of a certain order n, so that it is sufficient to consider only forces of polynomial type. By subsequent integration by parts, it can be shown that the Fourier transform $f(\omega)$ may be written as $f(\omega) = Ae^{i\omega a} + Be^{-i\omega a}$, where $A,B = \mp \Sigma_{j=0}^{n} [i^{j+1} f^{(j)}(\pm a)/\omega^{j+1}]$ and $A(B)$ corresponds to the upper (lower) sign. Therefore the bremsstrahlung spectrum $dI/d\omega$ consists of a polynomial part superimposed on an oscillating part. In this simple example the oscillating part has the frequency π/a. In real physical processes the frequency of the oscillations depends upon details of the acting force.

In a semiclassical approximation the radiated energy per phase-space element is given by [11]

$$2(2\pi)^3 \frac{d^3I}{d^3k} = |j_\mu^*(k) j^\mu(k)|, \tag{1}$$

where $k=(\omega,\vec{k})$ is the photon four-momentum and $j^{\mu}(k)$ is the Fourier transform of the classical four-current. Equation (1) is justified if the recoil of charged particles due to the bremsstrahlung emission can be neglected. This is equivalent to the condition $\omega \ll p_0$, where p_0 is the energy of the particles.

By using charge conservation, $k_{\mu}j^{\mu}(k)=0$, and neglecting the transverse components of $\vec{j}(k)$, which is a good approximation at high bombarding energies, one has

$$|j^{*}_{\mu}(k)j^{\mu}(k)|=\left(\frac{k_{\perp}}{\omega}\right)^2|j_z(k)|^2. \tag{2}$$

From Eqs. (1) and (2) it follows that

$$\frac{dI}{d\omega d\Omega}=\frac{k_{\perp}^2}{16\pi^3}|j_z(k)|^2. \tag{3}$$

Let us assume that photons are produced in microscopic binary collisions of pointlike particles which instantaneously change their velocities in each collision vertex. Then the explicit expression for $j^{\mu}(k)$ may be written as

$$j^{\mu}(k)=i\sum_i\ \sum_j\ e_j\left(\frac{p^{\mu}_{ij}}{k\cdot p_{ij}}-\frac{p^{\mu}_{i-1j}}{k\cdot p_{i-1j}}\right)e^{ik\cdot x_{ij}}, \tag{4}$$

where indices i and j count vertices and particles, respectively. The four-vector x_{ij} is the space-time position of the ith collision vertex of the jth particle, e_j is the charge of the latter. It is assumed that at $x=x_{ij}$ the jth particle four-momentum jumps from p_{i-1j} to p_{ij}. Equation (4) can easily be applied to inelastic particle collisions if one extends the definition of the charge $e_j \rightarrow e_{ij}$ and allow the charge to change at a vertex. For example, if some charged particle is produced at the vertex i then $e_{i-1j}\equiv 0$ and $e_{ij}\neq 0$.

The assumption of instantaneous binary collisions used in the derivation of Eq. (4), is fulfilled if the emitted bremsstrahlung photon is not able to resolve details of the microscopic scattering process. This in turn requires that the time scale of the photon emission, $\sim\omega^{-1}$, is much larger than the characteristic scattering time τ_s. If the particles interact via the strong interaction, $\tau_s \sim 1/m_{\pi}\sim 1$ fm/c, where m_{π} is the pion mass. In this case the above condition is fulfilled for photon energies $\omega \lesssim \tau_s^{-1}\sim 200$ MeV. At large enough bombarding energies the neglection of the recoil of the particles will then be trivially fulfilled. The approximations used in the derivations of Eqs. (1) and (4) are known as the *soft photon approximation* [12].

Assuming for simplicity that the particles move along the beam direction z, one immediately finds from Eqs. (3) and (4) that the emission of soft photons is suppressed if the particles are reaccelerated in the course of the reaction. The same phenomenon takes place if charges are produced and reabsorbed during a heavy-ion collision. By introducing a time cut one can decompose the current into parts having fixed but opposite signs of the acceleration or into parts corresponding to increasing and decreasing number of charged particles, respectively. It can be shown that the interference of the radiation from these two current components is destructive for soft photons.

The soft photon limit of Eq. (1) is independent of the collision dynamics, but depends only on the charged particles' velocities in the initial and final states of the reaction. In this case the sums over the incoming and outgoing particles can be replaced by integrals over the initial and final velocity distributions. Let us consider the soft-photon limit of Eq. (1) for the case of symmetric central heavy-ion collisions, assuming that the charges move along the beam axis. For sharp initial and final velocity distributions one finds

$$\lim_{\omega\rightarrow 0}\frac{dI}{d\omega d\Omega}=\frac{4Z^2\alpha(\beta_i^2-\beta_f^2)^2\sin^2\theta\cos^2\theta}{(2\pi)^2(1-\beta_i^2\cos^2\theta)^2(1-\beta_f^2\cos^2\theta)^2}. \tag{5}$$

Here $\beta_i(\beta_f)$ is the initial (final) velocity of charged particles, θ is the c.m. emission angle, Z is the total charge of each nucleus, and $\alpha=e^2/(4\pi\hbar c)$ is the QED fine structure constant. The right-hand side (RHS) of Eq. (5) exhibits the typical behavior of quadrupole radiation, which is a direct consequence of the symmetry of the considered system.

Using Eq. (5) it can be shown that the angle of maximum radiation equals

$$\theta_{\max}=\arccos\sqrt{\frac{1-(u_+ +u_-)-i\sqrt{3}(u_+ -u_-)}{2}},$$

with

$$u_{\pm}=\sqrt[3]{-\frac{\beta_i^2+\beta_f^2-\beta_i^2\beta_f^2}{8\beta_i^2\beta_f^2}\pm\sqrt{\left(\frac{-4+2\beta_i^2+2\beta_f^2-3\beta_i^2\beta_f^2}{4\beta_i^2\beta_f^2}\right)^3+\left(\frac{\beta_i^2+\beta_f^2+\beta_i^2\beta_f^2}{8\beta_i^2\beta_f^2}\right)^2}}.$$

Clearly for $\beta_i \gtrsim 0.9$ the angle $\theta_{\max}$ depends quite weakly on β_f (if β_f is not too close to β_i). To a good accuracy it may be assumed that $\beta_f \simeq 0$, which leads to

$$\theta_{\max}=\operatorname{arcctg}\gamma_i, \tag{6}$$

where $\gamma_i=(1-\beta_i^2)^{1/2}$. Substituting $\theta=\theta_{\max}$ into Eq. (5)

yields the following estimate for the height of the maximum in the photon angular distribution:

$$\lim_{\omega\to 0}\left.\frac{dI}{d\omega d\Omega}\right|_{\theta_{\max}}=\frac{Z^2\alpha(\beta_i^2-\beta_f^2)^2(2-\beta_i^2)^2}{(2\pi)^2(1-\beta_i^2)(2-\beta_i^2-\beta_f^2)^2}. \quad (7)$$

If $\beta_f\simeq\beta_i$ the exact value of $\theta_{\max}$ becomes smaller. In the case $\beta_f\simeq\beta_i\simeq 1$ one finds $\theta_{\max}\sim 1/(\sqrt{3}\gamma_i)$. At large bombarding energies the photons emitted in a heavy-ion collision are strongly peaked in forward and backward directions ($\theta_{\max}\sim 1/\gamma_i$) and, therefore, practically do not overlap in phase space. In this case the interference term between the projectile and target photons becomes negligible and the quadrupole spectrum may be well approximated by the sum of the dipole spectra generated by each nucleus. For pure dipole radiation we find $\theta_{\max}=\arccos\beta_i$ for $\beta_f\simeq 0$ and $\theta_{\max}\sim 1/(\sqrt{3}\gamma_i)$ for $\beta_i\simeq\beta_f\simeq 1$. Strictly speaking, however, using the approximation of dipole radiation in (symmetric) heavy-ion collisions [2,5] is not correct.

The same conclusion about the low sensitivity of the soft photon angular distribution to the projectile-target stopping also holds for broad final velocity distributions, provided that the mean final velocity is much smaller than β_i. In this case only the amplitude and not the angular distribution of the radiation is sensitive to the degree of stopping. This discussion shows that for a large range of nuclear stopping soft bremsstrahlung alone can not serve as a good tool to measure the impact parameter [2] since in the soft photon limit only the amplitude of the bremsstrahlung spectrum is affected by both the involved charge and the final velocity distribution. Moreover, the investigation of the soft photon spectrum [Eqs. (5) and (7)] shows that with increasing bombarding energy also the sensitivity of the amplitude on the final velocity becomes extremely weak for a large range of final velocities. For example, in the case of a Au+Au collision at RHIC energies ($y_i=\operatorname{artanh}\beta_i\simeq 5.4$) the amplitudes for the final c.m. rapidities $y_f=0$ and $y_f=3$ differ by less than 5%.

As is well known, scattering of particles exclusively along the beam direction excites only the $m=0$ multipole components of the radiation field. This implies that no photons are emitted in and transverse to the beam direction. Of course, transverse scattering or the loss of the projectile-target symmetry of the current (e.g., in peripheral collisions [13]) excite components with $m\neq 0$. As a consequence, nonvanishing radiation at $\theta\simeq 0$ and $\pi/2$ will appear [6].

Let us now consider the influence of the nuclear charge form factor on the photon spectra. At large bombarding energies particles move practically along the beam axis, and the transverse sizes of the colliding nuclei remain almost unchanged during the most violent initial stage of a heavy-ion collision. It is assumed for simplicity that the transverse form factor $F(k_\perp)$ can be factored, yielding approximately

$$\frac{dI}{d\omega d\Omega}\approx|F(k_\perp)|^2\left(\frac{dI}{d\omega d\Omega}\right)_0, \quad (8)$$

where $(dI/d\omega d\Omega)_0$ denotes the spectrum obtained for rodlike nuclei with zero transverse extension. This formula is well justified only for a certain class of charge density distributions (e.g., for a cylindrical shape, see Sec. III A). It becomes exact at very large bombarding energies, where $F(k_\perp)$ is given by the transverse Fourier transform of the nuclear thickness function [7]. The presence of the nuclear form factor $F(k_\perp)$ suppresses the photon yield at transverse photon momenta $k_\perp\gtrsim 1/R$, where R is the nuclear radius. Since $k_\perp=\omega\sin\theta$, the suppression becomes stronger for increasing photon energy or lager angles of emission with respect to the beam axis. As a result, with increasing photon energy the maxima of $dI/d\omega d\Omega$ appear to be shifted to smaller emission angles.

Another feature common to all models is that the compression of nuclear matter at intermediate stages of a heavy-ion reaction is correlated with the characteristic time of the heavy-ion collision. In general, larger times of the heavy-ion reaction correspond to larger intermediate densities and to smaller slopes of the spectra with respect to ω. Therefore, the measurement of these slopes may in principle provide some information about the compression achieved in a heavy-ion collision.

III. DYNAMICAL MODELS OF NUCLEAR COLLISIONS

A. Shock wave model

In the first model it is assumed that two plane shock waves moving with constant c.m. velocities, $\pm\beta_{\rm sh}$, develop at the moment of the first contact of the projectile and target nuclei. Within the shock wave model (SWM) it is postulated that the c.m. velocity of nuclear matter is zero behind the shock fronts, i.e., at $|z|<\beta_{\rm sh}t$. For simplicity the initial nuclei are treated as cylinders with effective radius R and length $2R/\gamma_i$. One can write the relation $\varrho_0\gamma_i(2R/\gamma_i)\pi R^2=A$, where $\varrho_0=0.17$ fm^{-3} is the normal nuclear density and A is the atomic number of the colliding nuclei. In the case of Au nuclei, $R\simeq 0.98A^{1/3}$ fm$\simeq 5.7$ fm. This is slightly less than the geometrical value $R_g\simeq 1.12A^{1/3}$ fm$\simeq 6.5$ fm.

Before the collision, at $t<0$, the longitudinal component of the electromagnetic current can be written as

$$j_z(t,\vec{r})=\frac{eZ}{A}\varrho_0\gamma_i\beta_i\Theta(R-r_\perp)\times[\Theta(\beta_i t-z)\Theta(z-z_i(t))-(z\to -z)]. \quad (9)$$

Here $\Theta(x)\equiv\frac{1}{2}(1+\operatorname{sgn}x)$, and $z_i(t)=-2R/\gamma_i+\beta_i t$, $\vec{r}_\perp(z)$ are the transverse (longitudinal) components of $\vec{r}$ with respect to the beam axis. The first term and the second term in the square brackets of Eq. (9) correspond to the projectile and target nucleus, respectively. The shock fronts, appearing at $t=0$, reach the rear sides of the colliding nuclei at $t=\tau\equiv 2R/\gamma_i(\beta_i+\beta_{\rm sh})$. The explicit expression for j_z at the intermediate stage, i.e., for $0<t<\tau$, is given by Eq. (9) with the replacement $\Theta(\beta_i t-z)\to\Theta(-\beta_{\rm sh}t-z)$. The moment $t=\tau$ is found by solving the equation $z_i(\tau)+\beta_{\rm sh}\tau=0$. At $t>\tau$ compressed matter starts to expand into the vacuum. We neglect the photon production at this less violent stage of the reaction, assuming that $j_z(t,\vec{r})$ vanishes for $t>\tau$.

In accordance with Eq. (1), the spectrum of bremsstrahlung photons is determined by the Fourier transform of the four-current $j^{\mu}(k)$. After introducing the transverse density form factor of the initial nuclei

$$F(k_{\perp})=\frac{1}{\pi R^2}\int d^2r_{\perp}e^{-i\vec{k}_{\perp}\vec{r}}\Theta(R-r_{\perp})=\frac{2J_1(k_{\perp}R)}{k_{\perp}R}, \tag{10}$$

one arrives at the expression

$$j_z(k)=ZeF(k_{\perp})\beta_i\left[\frac{1-e^{i\omega\tau(1+\beta_{\rm sh}\cos\theta)}}{(\omega-\beta_i k_z)\omega\tau(1+\beta_{\rm sh}\cos\theta)}+\frac{e^{i\omega\tau(1-\beta_{\rm sh}\cos\theta)}-1}{(\omega+\beta_i k_z)\omega\tau(1-\beta_{\rm sh}\cos\theta)}\right]. \tag{11}$$

Equivalently, the Fourier transformed current (11) can be calculated directly using Eq. (4), assuming homogeneously charged nuclear matter and replacing the sum by an integral. The space-time positions of the vertices x_{ij} coincide in this calculation with the positions of the shock fronts.

Using Eqs. (3) and (11) yields the final result (the respective formula given in Ref. [14] is incorrect)

$$\frac{dI}{d\omega d\Omega}=\alpha\left(\frac{Z\beta_i\sin\theta}{\pi\omega\tau}\right)^2F^2(\omega\sin\theta)\left\{\frac{\sin^2[\omega\tau(1+\beta_{\rm sh}\cos\theta)/2]}{(1-\beta_i\cos\theta)^2(1+\beta_{\rm sh}\cos\theta)^2}+\frac{\sin^2[\omega\tau(1-\beta_{\rm sh}\cos\theta)/2]}{(1+\beta_i\cos\theta)^2(1-\beta_{\rm sh}\cos\theta)^2}\right.$$

$$\left.+\frac{\cos(\omega\tau\beta_{\rm sh}\cos\theta)[\cos\omega\tau-\cos(\omega\tau\beta_{\rm sh}\cos\theta)]}{(1-\beta_i^2\cos^2\theta)(1-\beta_{\rm sh}^2\cos^2\theta)}\right\}. \tag{12}$$

This formula contains only one model parameter—the shock wave velocity $\beta_{\rm sh}$. It determines the duration of the collision and the achieved compression of nuclear matter. Strong shocks with large energy densities of the stopped matter correspond to $\beta_{\rm sh}\ll 1$. On the other hand, from the baryon current conservation, it can be shown that in the limit $\beta_{\rm sh}\to 1$ the compression of matter behind the shock front ϱ/ϱ_0 approaches its minimal value $\sqrt{(1+\beta_i)/(1-\beta_i)}$. The soft photon limit clearly corresponds to $\omega\tau\ll 1$. It may be verified that the soft photon limit is reached either for ω or $\tau\to 0$. In the lowest order the photon spectrum given by Eq. (8) is obtained, where $(dI/d\omega d\Omega)_0$ is equal to the RHS of Eq. (5) with $\beta_f=0$. As expected, in this limit the photon spectrum does not contain any information about the parameters of the shock waves.

B. Degradation length model

In the second model we treat each nucleus as a set of n test particles with the charge $e(Z/n)$ moving along the beam axis. In the ground state of a nucleus the test particles are homogeneously distributed. It is assumed that these particles collide when their trajectories intersect in the (t,z) plane. The stopping law for the colliding matter is determined by the rule how the slopes of the trajectories change at the collision vertices. In the model we have applied a simple stopping law [15]

$$\frac{dp}{dz}=-\frac{p}{\Lambda}, \tag{13}$$

where z is the distance in nuclear matter covered by the test particles and Λ is the so-called degradation length.

To implement Eq. (13) into the degradation length model (DLM1) we postulate that the change of momentum of each test particle is determined by its number of collisions, i.e., by the number of trajectories crossed by the test particle during its path in nuclear matter. In this model we neglect the transverse sizes of the colliding nuclei and locate all test particles along the beam axis. The computational procedure is based on the finite difference equation

$$p(z+\Delta z)=p(z)-p(z)\frac{\Delta z}{\Lambda}. \tag{14}$$

The LHS of Eq. (14) gives the momentum after the test particle collision, Δz is a fixed value determined by the distance traveled by the test particles in the ground state of the nucleus. The vertex positions and velocities entering Eq. (4) are provided by the construction rule for the trajectories. In the limit $n\to\infty$ we again get a homogeneously charged matter and unphysical oscillations in the photon spectra caused by a finite number of test particles are washed out. The bremsstrahlung spectrum is obtained by substituting Eq. (4) into Eq. (1).

Figure 1 shows the trajectory representations of the SWM and the DLM1. Dynamical differences between these two stopping scenarios are clearly visible. One can see that in the SWM the stopping time is determined by $\beta_{\rm sh}$ and is independent of the degree of stopping whereas in the DLM1 this time depends on the degree of stopping.

In the extended degradation length model (DLM2) we generalize the DLM1 and consider the colliding nuclei as homogeneously charged spheres represented by test particles. Binary collisions of test particles are treated in the same way as above. The final velocity of each test particle is

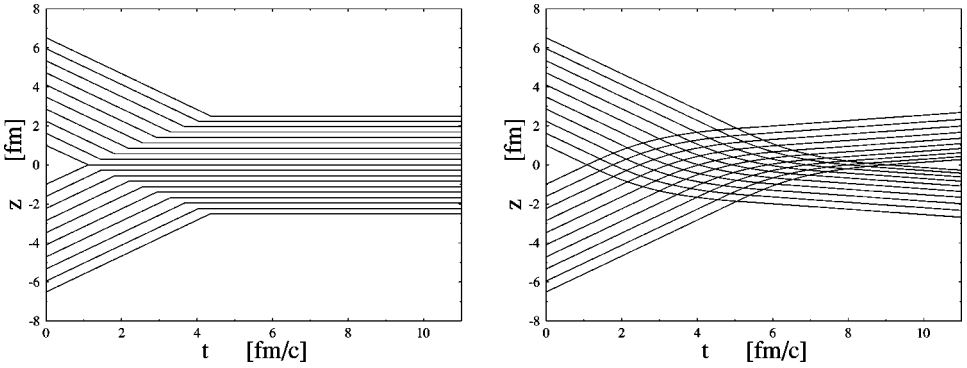

FIG. 1. Trajectory representation of the shock wave model (left) and the degradation length model (right). Both calculations represent a central Au+Au collision at AGS energy (10.6*A*GeV).

again determined by the distance traveled in nuclear matter, but this distance now depends on the transverse separation from the nuclear center. Therefore, spherical shapes of the colliding nuclei give rise to a broadening of the final velocity distribution and to a more complex structure of the current. On the contrary, the assumption of a cylindrical nuclear shape adopted by the SWM leads to a sharp final velocity distribution ($\beta_f=0$). As discussed in Sec. II, the broadening of the final velocity distribution leads to almost the same shapes of soft photon spectra, but reduces the amplitude of the photon yield.

The influence of both the degree of transparency and the broadening of the final velocity distribution due to the spherical geometry of the nuclei is demonstrated in Fig. 2. Since stopping is effectively reduced due to the spherical shape of the nuclei, the radiated energy is also reduced. The comparison of spectra predicted by DLM1 and DLM2 indeed confirms this conclusion. In accordance with the previous discussion, the sensitivity of the photon angular distribution to the final velocity distribution is low for small final velocities, i.e., in the limit $\Lambda\rightarrow 0$. In the case of weak stopping (large Λ) the maxima of the angular distribution shift to smaller angles. Calculations show that for $\Lambda\lesssim 5$ fm the angles of maximum radiation agree well with Eq. (6). Within the DLM1 the heights of the maxima are well explained by Eq. (7) with the final velocity obtained from Eq. (13). Alternatively, Eq. (7) may be used to estimate the mean final velocity in the DLM2.

C. Transport model

In the present paper we also consider the microscopic transport model UrQMD [16]. In this approach the whole history of the heavy-ion collision enters the photon spectrum. This allows to take into account also the contributions from the late stages of the collision.

To demonstrate how the microscopic currents are treated in the model it is instructive to rewrite Eq. (4) as

$$j^{\mu}(k)=i\sum_i \sum_j \hat{e}_j \frac{p_{ij}^{\mu}}{k\cdot p_{ij}} e^{ik\cdot x_{ij}}, \tag{15}$$

where the notation

$$\hat{e}_j=\begin{cases} e_j & \text{if } j \text{ corresponds to an incoming particle,} \\ -e_j & \text{if } j \text{ corresponds to an outgoing particle} \end{cases} \tag{16}$$

is introduced. The sum runs over all charged particles j and their collision vertices i. Such a procedure is applied to any kind of vertex (elastic or inelastic collisions with arbitrary number of produced particles) as well as for decays of unstable particles or strings. Influence of mean-field potentials producing smooth bending of particle trajectories is neglected. Here it is assumed that hard binary collisions result in much stronger deceleration of the particles.

An important background contribution to photon spectra comes from $\pi^0\rightarrow\gamma\gamma$ decays. In the UrQMD model the contribution of these decays can be calculated directly. In this calculation it was assumed that π^0 mesons decay isotropically in their rest frame.

To reduce the statistical fluctuations, the calculated spectrum was averaged over a large number of events.

IV. COMPARISON OF PHOTON SPECTRA

In this section we compare the model predictions in the case of central Au+Au collisions at the AGS bombarding energy. Since photon radiation in a symmetric heavy-ion collision is symmetric in the c.m. frame with respect to $\theta=\pi/2$, the results are shown only for $0\leqslant\theta\leqslant\pi/2$.

Figure 3 shows the angular distribution of bremsstrahlung

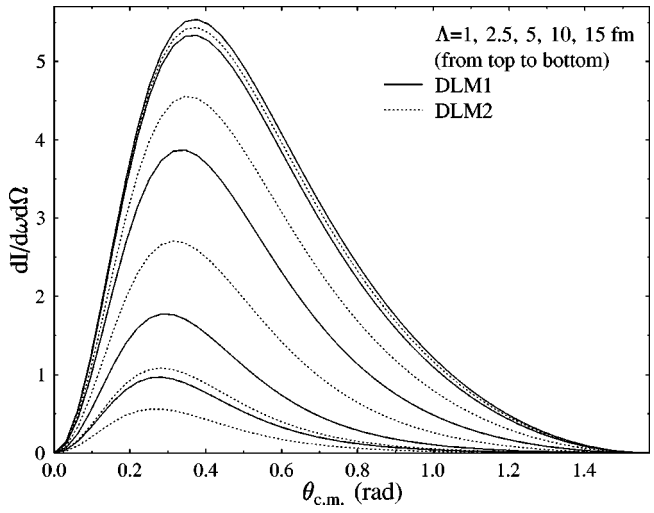

FIG. 2. Angular distributions of soft photon bremsstrahlung ($\omega=1$ MeV) in a central Au+Au collision at AGS energy predicted by the degradation length model with and without transverse nuclear extension.

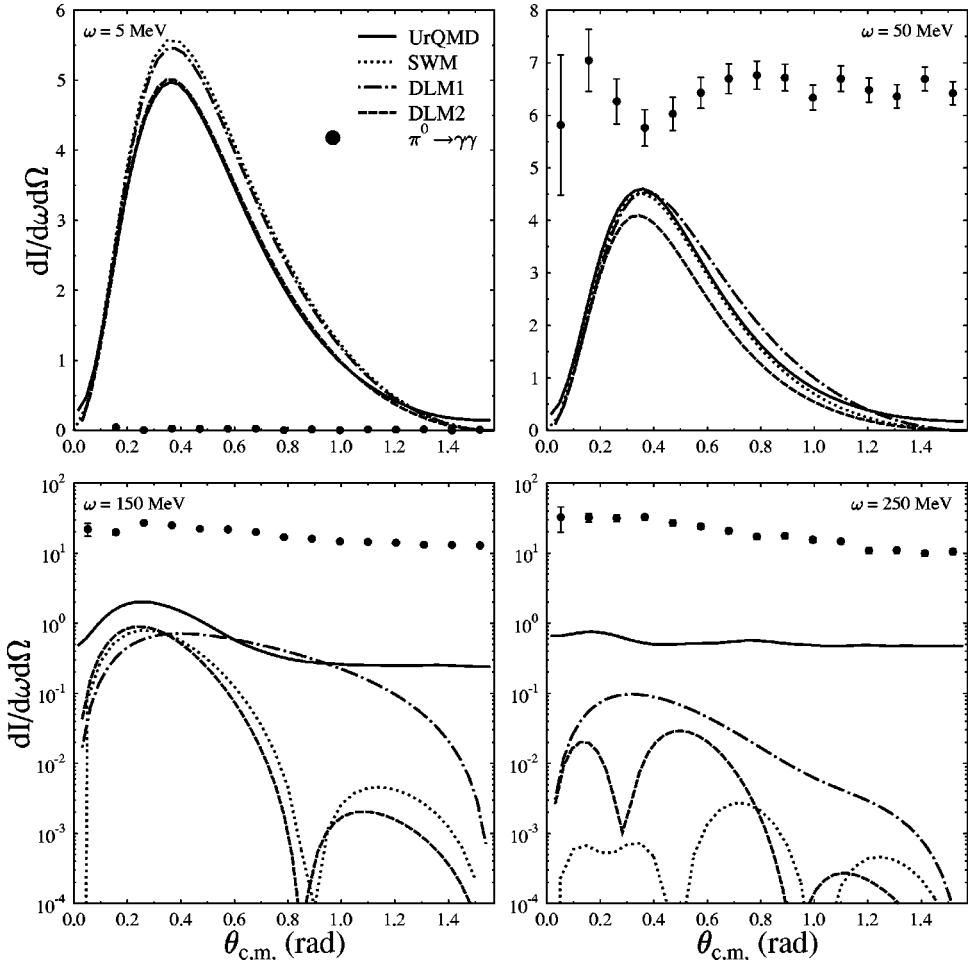

FIG. 3. Angular distribution of bremsstrahlung spectra predicted by different models for a central 10.6*A* GeV Au+Au collision at the photon energies $\omega=5$, 50, 150, and 250 MeV. The dots show the contribution of $\pi^0\rightarrow\gamma\gamma$ decays. Note that the vertical scale in the last two figures is logarithmic.

photons at the AGS bombarding energy 10.6*A* GeV. Four different photon energies are considered. The parameters of the models are $y_{\rm sh}=\operatorname{artanh}\beta_{\rm sh}=1$ (SWM) and $\Lambda=2$ fm (DLM1 and DLM2). In the considered reaction such a degradation length corresponds to rather strong stopping.

At $\omega=5$ MeV the SWM and the DLM1 overestimate the bremsstrahlung yield as compared to the UrQMD calculation. The inclusion of a realistic nuclear shape, however, results in a good agreement of the DLM2 with the UrQMD model. This agreement favors a strong stopping at intermediate stages of a central Au+Au collision at AGS energy. Note that the degradation length Λ entering the model calculation $\Lambda=2$ fm corresponds to $\Lambda'\simeq 5.2$ fm in the laboratory frame. The latter is close to the value obtained by fitting *pA* data [17].

All simple models incorporating only the stopping phase of a heavy-ion collision underestimate the radiation in forward ($\theta\simeq 0$) and transverse ($\theta\simeq\pi/2$) direction to the beam. This is especially visible at larger ω's. As will be shown below, the additional contributions originate mainly from the late stages of the heavy-ion collision. Indeed, contributions from the expansion phase of the collision, and bremsstrahlung produced in rescatterings with newly produced particles are disregarded in the SWM, DLM1, and DLM2. It should be noted that at the AGS energy the transverse scattering of particles (see Ref. [6]) gives only small contributions and cannot explain the above-mentioned disagreement.

We find that up to $\omega=50$ MeV all models predict roughly the same angular distributions. In this case photon spectra are dominated by the quadrupolar radiation produced in the course of mutual deceleration of the colliding nuclei. As discussed above, bremsstrahlung photons with energies less than or of the order $1/\tau$, where τ is the characteristic time of the heavy-ion collision, cannot resolve the detailed structure of the current. Estimating τ by the nuclear passage time we have in the case of a Au+Au collision at the AGS energy $\tau\sim 2R/(\gamma_i\beta_i)\sim(50\ \ {\rm MeV})^{-1}$. On the other hand, according to Fig. 3, the simple models predict a more rapid decrease with ω than the UrQMD model.

Within the SWM and the DLM2 the decrease of the photon yield at $\omega\gg 1/\tau$ is determined mainly by the nuclear form factor. The shift of maximum radiation to smaller angles (see Sec. II) is clearly visible already at $\omega=150$ MeV. As compared to the DLM1, the inclusion of the form factor in the DLM2 leads to the appearance of additional maxima. The predictions of the SWM and the DLM2 are rather close, although these models are based on very different dynamical scenarios. The SWM predicts additional maxima with comparable heights and locations. However, by using Eq. (12) it is easy to show that additional maxima appear in this model for any $\beta_{\rm sh}\neq 0$ even if the transverse size of the nuclei is neglected, i.e., by assuming $F(k_\perp)\equiv 1$.

At $\omega = 250$ MeV angular distributions calculated within the simple stopping models and the UrQMD model differ considerably both in shapes and amplitudes of the photon spectra. At this energy additional maxima appear also in the UrQMD model. However, these maxima are much smoother than in the SWM and the DLM (note the logarithmic scale on the vertical axis).

The freedom in the choice of model parameters is limited by the assumed stopping law. For instance, it is not possible to improve the agreement between the DLM2 and the UrQMD model at higher photon energies (by chosing a smaller Λ) without losing the agreement for soft photons.

As mentioned above, the spectra predicted by the SWM and the DLM1 and DLM2 decrease faster with respect to ω as compared to the spectrum calculated within the UrQMD model. Special analysis shows that contrary to the discussion of Sec. II this behavior is not determined by the collision times assumed in these models. Indeed, at the AGS energy the spectrum predicted by the SWM decreases faster with ω than the DLM2 although the characteristic collision time of the DLM2 ($\tau \sim 8$ fm/c) is more than twice as large as compared to the SWM ($\tau \sim 3.5$ fm/c). A rough estimate shows that the collision time of the UrQMD model is of the order of 6 fm/c.

A more detailed study of the photon spectra has been performed within the UrQMD model. Figure 4 shows the different components of the bremsstrahlung spectra generated in UrQMD events. A time cut at $t_{\rm cut} \simeq 6$ fm/c has been introduced to separate the contributions from the early stopping phase and the late stages of the collision. This time cut is close to the passage time of the gold nuclei. The contribution of the stopping phase ($t < t_{\rm cut}$) has the familiar quadrupolar shape and is well understood within the SWM and DLM. Bremsstrahlung from the late stages is nearly isotropic and is smaller for soft photons. This is understandable since the charge-current varies smoothly with time at these stages of the collision. The characteristics of the bremsstrahlung component from $t > t_{\rm cut}$ do not contradict the conclusion made in Ref. [18] that local equilibration is achieved in 10.6A GeV central Au+Au collisions at $t > 10$ fm/c within a volume of $(5 \text{ fm})^3$. Apparently, deviations from angular isotropy can be explained by a nonspherical shape of the dense central region elongated in the beam direction [18].

The interference between the bremsstrahlung photons from the two considered stages indicates to which extent it is justified to study the radiation from the different stages separately. The noticeable negative interference at small photon energies probably follows from a reacceleration of charges at late stages of the collision. It may serve as a signal of the final expansion of the compressed matter. Suppression of soft photons due to reacceleration of charges at late stages was found also in the Landau fluid-dynamical model [8]. Due to the noticeable interference the bremsstrahlung models considering only the stopping phase of a heavy-ion collision may underestimate the stopping power of nuclear matter if such models are used to fit observed soft photon spectra.

Figure 5 represents the energy spectra of photons predicted with the SWM, DLM2, and UrQMD model at the angle of maximum radiation given by Eq. (6). One can see a

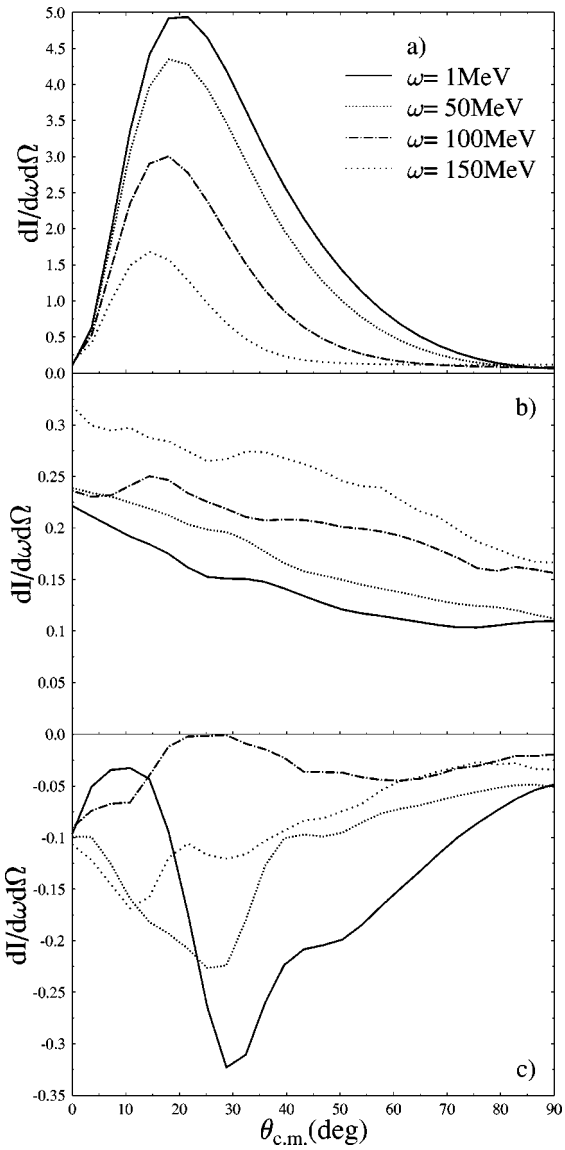

FIG. 4. Contributions to the bremsstrahlung spectra from different stages of a central Au+Au collision at AGS energy: (a) deceleration stage ($t < t_{\rm cut}$), (b) expansion stage ($t > t_{\rm cut}$), and (c) interference of (a) and (b).

qualitatively different behavior of the spectra predicted by simple models and the UrQMD model at large ω's. In the considered case of the AGS energy the SWM and DLM2 noticeably underestimate the UrQMD predictions at $\omega \gtrsim 150$ MeV. Moreover, the UrQMD spectrum slightly increases with energy at $\omega \gtrsim 200$ MeV. Apparently, such a behavior also originates from the late stages of the reaction. The high-energy part of Fig. 5 has only a methodical interest. As noted above, the soft-photon approximation is violated for photons with c.m. energies $\omega \gtrsim 200$ MeV. The results for hard photons are shown for the sake of comparison between the UrQMD and the simple models.

As a result, one may conclude that nonsoft domains of the photon spectra cannot be studied realistically without an explicit treatment of the late stages of a heavy-ion collision. On the other hand, the presence of the π^0 background highly

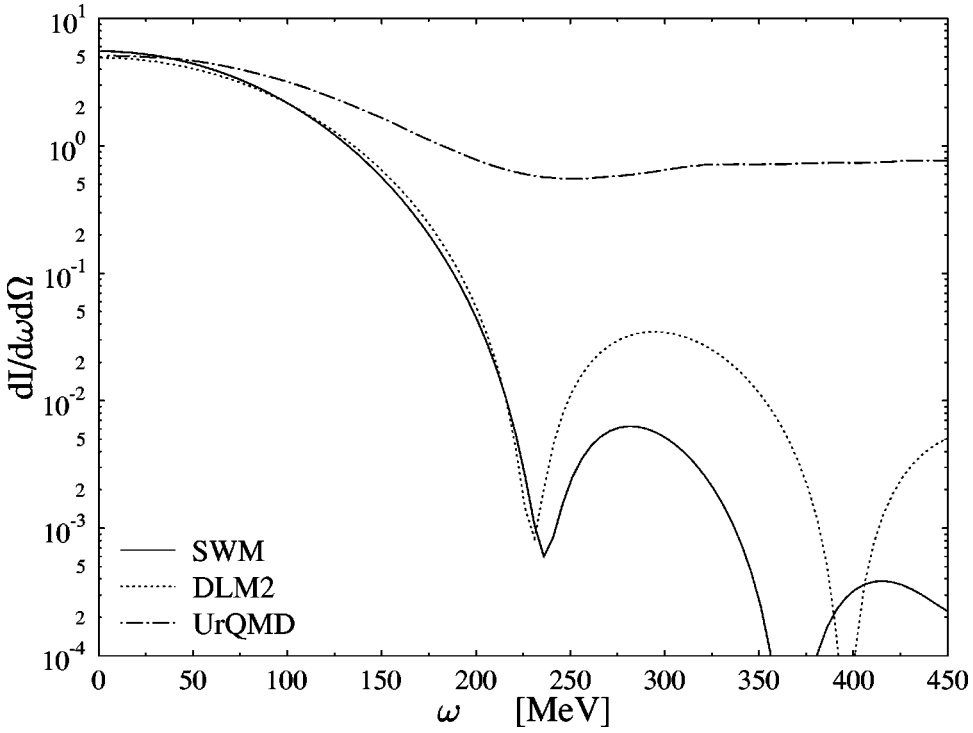

FIG. 5. Energy spectra of bremsstrahlung photons in a 10.6*A* GeV central Au+Au collision.

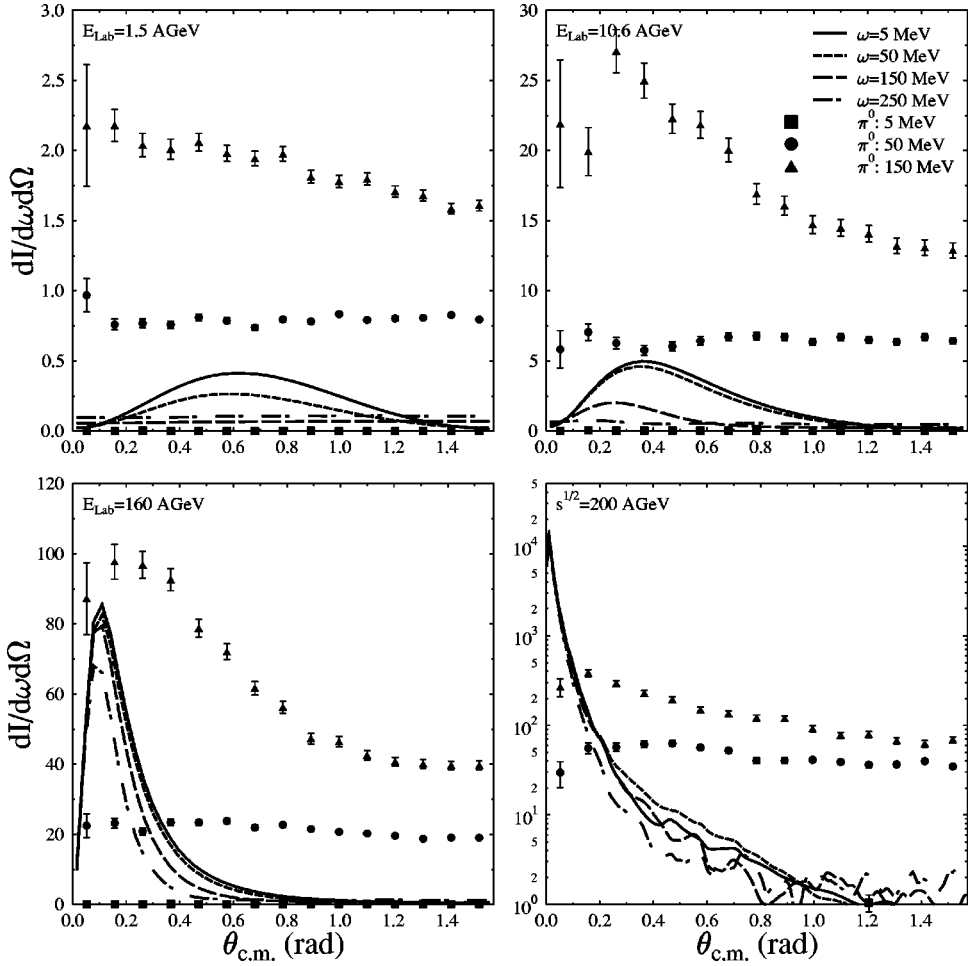

FIG. 6. Bremsstrahlung and π^0 decay spectra predicted by the UrQMD model for central Au+Au collisions at the SIS, AGS, SPS, and RHIC energies.

complicates the measurements of bremsstrahlung spectra at large photon energies.

This is illustrated in Fig. 6 which shows the photon spectra predicted by the URQMD model at different bombarding energies from SIS to RHIC. In accordance with the general discussion the photon spectra become more forward peaked with increasing initial energy. As one can see in Figs. 3 and 6, the background of electromagnetic decays of π^0 mesons at the AGS energy exceeds the coherent photon yield already at $\omega \gtrsim 50$ MeV. At the SPS and RHIC energies the coherent bremsstrahlung remains important even for higher ω's (at small emission angles).

V. CONCLUSIONS

We have discussed general properties of the coherent bremsstrahlung spectra common to any model of heavy-ion collisions. The comparison of four different models shows that the photon spectra are sensitive to the dynamics of the projectile-target stopping only in the nonsoft regime. We have shown, however, that even at higher photon energies different models may generate similar photon spectra. Photons produced in the stopping phase of a heavy-ion collision yields a dominant contribution to the bremsstrahlung at small photon energies. As shown within the microscopic model, the radiation of nonsoft photons comes mainly from later (expansion) stages.

The soft photon yield can provide some information about the degree of stopping. Soft photon spectra at ultrarelativistic bombarding energies, however, reveal a rather weak sensitivity to the final velocities of secondary particles.

At the AGS and lower bombarding energies the background of π^0 decays is relatively large even for soft photons. According to our analysis, measurements of the soft photon spectra can hardly provide precise information about characteristics of nuclear stopping.

In principle, the spectral slopes may be used to estimate the collision time or the compression achieved in the heavy-ion reaction. The comparison of different models showed, however, that the dependence of the spectra on the photon energy is highly model-dependent and thus does not provide reliable information about the collision time and the compression. Furthermore, the analysis of microscopic calculations performed within the UrQMD model shows that the shapes of the coherent bremsstrahlung spectra as functions of the photon energy are strongly sensitive to the late stages of the reaction.

It is shown by general analysis that oscillations of the energy spectra always appear in models assuming a finite time of the collision and, therefore, may be an artifact of a simplified description. The use of these oscillations to extract properties of matter in nuclear collisions is only possible within certain simplified models [14]. Moreover, these oscillations are strongly smoothened if one takes into account the photon radiation from the late expansion stages.

ACKNOWLEDGMENTS

This work was supported by the Graduiertenkolleg Theoretische und Experimentelle Schwerionenphysik, DFG, and by the RFBR Grant No. 00-15-96590.

[1] J. Kapusta, Phys. Rev. C **15**, 1580 (1977).
[2] J.D. Bjorken and L. McLerran, Phys. Rev. D **31**, 63 (1985).
[3] J. Thiel, T. Lippert, N. Grün, and W. Scheid, Nucl. Phys. **A504**, 864 (1989).
[4] T. Lippert, J. Thiel, N. Grün, and W. Scheid, Int. J. Mod. Phys. A **29**, 5249 (1991).
[5] A. Dumitru, L. McLerran, H. Stöcker, and W. Greiner, Phys. Lett. B **318**, 583 (1993).
[6] U. Eichmann and W. Greiner, J. Phys. G **23**, L65 (1997).
[7] S. Jeon, J. Kapusta, A. Chikanian, and J. Sandweiss, Phys. Rev. C **58**, 1666 (1998).
[8] J. Kapusta, and S.M.H. Wong, Phys. Rev. C **59**, 3317 (1999).
[9] V. Koch, B. Blättel, W. Cassing, and U. Mosel, Phys. Lett. B **236**, 135 (1990).
[10] J.D. Jackson, *Classical Electrodynamics* (Wiley, New York, 1983).
[11] C. Itzykson and J.-B. Zuber, *Quantum Field Theory* (McGraw-Hill, New York, 1980).
[12] F. Low, Phys. Rev. **110**, 974 (1958).
[13] D. Vasak, Phys. Lett. B **176**, 276 (1986).
[14] C. Bertulani, L. Mornas, and U. Ornik, International Workshop on Models of Hadrons, Sao Paulo, 1994, hep-ph/9412303.
[15] R.C. Hwa, Phys. Rev. Lett. **52**, 492 (1984).
[16] S.A. Bass *et al.*, Prog. Part. Nucl. Phys. **41**, 225 (1998).
[17] L.P. Csernai, and J.I. Kapusta, Phys. Rev. D **31**, 2795 (1985).
[18] L.V. Bravina *et al.*, Phys. Lett. B **434**, 379 (1998).